Drag force on a moving impurity in a spin-orbit-coupled Bose-Einstein condensate

Pei-Song He,[1,2] Yao-Hui Zhu,[1] and Wu-Ming Liu[2]

[1]*School of Science, Beijing Technology and Business University, Beijing 100048, China*

[2]*Beijing National Laboratory for Condensed Matter Physics, Institute of Physics, Chinese Academy of Sciences, Beijing 100190,China*

(Received 9 December 2013; revised manuscript received 24 February 2014; published 13 May 2014)

We investigate the drag force on a moving impurity in a spin-orbit-coupled Bose-Einstein condensate. We prove rigorously that the superfluid critical velocity is zero when the impurity moves in all directions but one, in contrast to the case of liquid helium and superconductor, where it is finite in all directions. We also find that when the impurity moves in all directions except the two special ones, the drag force has nonzero transverse component with a small velocity. When the velocity becomes large and the states of the upper band are also excited, the transverse force becomes very small due to opposite contributions of the two bands. The characteristics of the superfluid critical velocity and the transverse force are results of the order-by-disorder mechanism in spin-orbit-coupled boson systems.

DOI: 10.1103/PhysRevA.89.053615 PACS number(s): 03.75.Kk, 03.75.Mn, 05.30.Jp

I. INTRODUCTION

Spin-orbit coupling (SOC) plays a crucial role in many physical systems ranging from nuclei and atoms to quantum spin Hall effect and topological insulators [1–4]. An artificial external non-Abelian gauge field coupled to neutral atoms of different hyperfine states can be engineered by controlling atom-light interactions [5–8]. Recently, Bose-Einstein condensates (BECs) with SOC as well as spin-orbit-coupled degenerate Fermi gases have been realized experimentally [9–13]. It provides physicists with a new platform to study the effects of SOC in many-body systems. A plenty of researches have been done on the properties of the BEC with SOC, including the ground-state phases [14–19], fluctuations above the ground state [20–23], and spin-orbit-coupled BECs with other cold-atom techniques, such as dipole-dipole interactions, optical lattices, and rotating traps [24–28].

One peculiar phenomenon intimately related to BEC is superfluidity, which was successfully explained by Landau [29]. According to the theory, there exists a critical velocity v_c with a finite value for an impurity moving in a superfluid, beyond which the impurity experiences a drag force. The Landau criterion has been confirmed in experiments using ions in superfluid ^{4}He [30] or an optical spoon in a gaseous Bose-Einstein condensate [31].

Landau's analysis cannot be directly applied to the case with a spin-orbit-coupled BEC, since it requires the system to be invariant under Galilean transformation, which is not satisfied when SOC exists. The low-energy excitations of a spin-orbit-coupled BEC are anisotropic Goldstone modes and spin waves; both are softer than the phonon in liquid helium. This may have profound effects on the superfluid critical velocity of the condensate. Moreover, the drag force experienced by the mobile impurity probably has exotic characteristics. In addition to the above-mentioned anisotropy of the BEC system and the existence of spin waves, the eigenfunctions of a free-boson system with SOC have a definite helicity, which are opposite for states in the lower and upper bands. These properties may lead to a transverse force even for a pointlike impurity. Since the upper band plays a role only when the impurity moves fast enough, the effects of the two-band structure on the drag force are also need to be clarified. In this article, we investigate the superfluidity of a spin-orbit-coupled BEC through its effects on an impurity which moves in it. We calculate analytically the drag force experienced by the impurity and also the superfluid critical velocity of the condensate.

This paper is organized as follows: Section II gives the model for a mobile impurity in a spin-orbit-coupled BEC. We use a time-dependent Gross-Pitaevskii equation to calculate the drag force experienced by the impurity. In Sec. III, the superfluid critical velocity and the drag force are given in detail. Section IV is a summary of this work.

II. MOTION OF AN IMPURITY IN SPIN-ORBIT-COUPLED BEC

We consider the motion of a pointlike impurity in a two-dimensional Rashba spin-orbit-coupled plane-wave BEC at zero temperature, as shown in Fig. 1. In the figure, F_L and F_T are longitudinal and transverse components of the drag force experienced by the impurity. One of the possible realizations of this scenario could be the scattering of heavy neutral molecules by the condensate.

A. An impurity moves in a spin-orbit-coupled BEC

We use a δ-function potential to describe the interaction between the pointlike impurity and the bosons in the condensate. The Hamiltonian for an impurity moving with a constant velocity $\mathbf{v}$ in the BEC is written as

$$\begin{aligned}\hat{H} = &\int d^2\mathbf{r}\hat{\Psi}^+(\mathbf{r},t)\left[-\frac{\hbar^2}{2m}\nabla^2 - \mu - 2i\hbar\lambda\nabla\cdot\boldsymbol{\sigma}\right]\hat{\Psi}(\mathbf{r},t)\\ &+\int d^2\mathbf{r}\delta(\mathbf{r}-\mathbf{v}t)[g_{i\uparrow}\hat{n}_\uparrow(\mathbf{r},t)+g_{i\downarrow}\hat{n}_\downarrow(\mathbf{r},t)]\\ &+\frac{1}{2}\int d^2\mathbf{r}[g_{\uparrow\uparrow}\hat{n}_\uparrow(\mathbf{r})^2+2g_{\uparrow\downarrow}\hat{n}_\uparrow(\mathbf{r})\hat{n}_\downarrow(\mathbf{r})+g_{\downarrow\downarrow}\hat{n}_\downarrow(\mathbf{r})^2].\end{aligned} \tag{1}$$

In Eq. (1), $\hat{\Psi}(\mathbf{r},t) = [\hat{\psi}_\uparrow(\mathbf{r},t),\hat{\psi}_\downarrow(\mathbf{r},t)]^T$ are time-dependent two-component boson field operators [9], where m is the mass

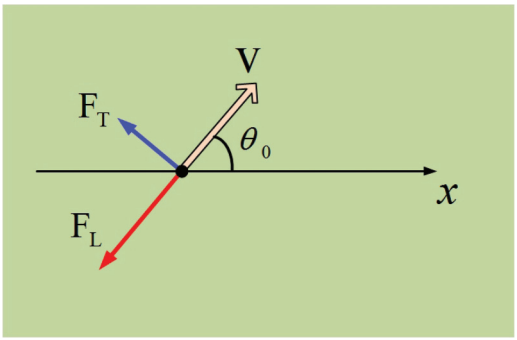

FIG. 1. (Color online) A pointlike impurity moves with velocity **v** in a two-dimensional spin-orbit-coupled Bose-Einstein condensate. The x direction is the principal direction of the plane-wave condensate. F_L and F_T are the longitudinal and transverse components of the drag forces experienced by the impurity.

of the atoms, λ is the strength of SOC, and μ is the chemical potential of the bosons.

In a free-boson system with Rashba SOC as in Eq. (1), the ground states compose a ring with $|\mathbf{k}| = \lambda$ in momentum space. The quantum fluctuations induced by particle-particle interactions will lift the macroscopic degeneracy. In this article, we use $g_{\uparrow\uparrow} = g_{\uparrow\downarrow} = g_{\downarrow\downarrow}$ for simplicity. In this case, due to the mechanism of order by disorder, the bosons condense on one point of the ring in momentum space [which we set as $\mathbf{k}_0 = (-\lambda,0)$] and result in a plane-wave condensate [19,32,33]. It has been proved that the condensate is stable against quantum fluctuations in both two and three dimensions [33–36]. Our calculations can be extended straightforwardly to the systems with $g_{\uparrow\uparrow}g_{\downarrow\downarrow} > g_{\uparrow\downarrow}^2$, in which the condensate also has plane-wave order. But the case with $g_{\uparrow\uparrow}g_{\downarrow\downarrow} < g_{\uparrow\downarrow}^2$ is more complicated [36,37], and it will be left to future considerations.

$g_{i\uparrow}$ and $g_{i\downarrow}$ in Eq. (1) are the strengths of the interactions between the impurity and bosons with pseudospins $\uparrow$ and $\downarrow$, respectively. For simplicity, we shall assume $g_{i\uparrow} = g_{i\downarrow}$ in this work.

The size effects of the impurity are neglected in Hamiltonian (1). Experimentally, it requires the dimension of the impurity to be much smaller than the coherence length ξ of the condensate. Otherwise, the situations will be much more complicated. First, the plane-wave condensate is anisotropic. When an impurity with a large size moves in an anisotropic fluid, since the properties of the fluid on different points of the impurity's surface usually differ, it is natural that the impurity will experience a transverse drag force [38–40]. In addition, there will be vortices excited in the condensate [41]. In a spin-orbit-coupled BEC, the characteristics of the vortices generally differ from those in cases without SOC [42–47]. In this paper, we focus on the least effects induced by the motion of a pointlike impurity in a spin-orbit-coupled BEC. The size effects of the impurity will be left to future considerations.

B. Drag forces and the Landau criterion in a spin-orbit-coupled BEC

Due to the absence of Galilean invariance in the spin-orbit-coupled BEC, the dynamical properties of the condensate are reference frame dependent [48,49]. So in our situation we have to choose the one with a static condensate.

We assume weak quantum fluctuations induced by the particle-particle interactions, as is usual in ultracold atom gas experiments. We also assume the impurity interacts weakly with the condensate. Under these assumptions, the dynamics of the boson fields $\Psi(\mathbf{r},t)$ can be well described by a time-dependent Gross-Pitaevskii (GP) equation,

$$i\hbar\partial_t\Psi = [-\nabla^2 - \mu - 2i\lambda\nabla\cdot\boldsymbol{\sigma} + g_i\delta(\mathbf{r}-\mathbf{v}t) + g|\Psi|^2]\Psi. \tag{2}$$

We neglect the possibility of exciting vortices by the pointlike impurity. Quantum fluctuations are created over the condensate by both the boson-boson and boson-impurity interactions. The full form of the boson fields are written as [50,51]

$$\Psi(\mathbf{r},t) = \sqrt{\rho_0+\delta\rho}\,e^{-i\lambda x + i\delta\theta}\begin{bmatrix}\cos(\frac{\pi}{4}+\delta\phi)e^{-i\frac{\delta\xi}{2}}\\ \sin(\frac{\pi}{4}+\delta\phi)e^{i\frac{\delta\xi}{2}}\end{bmatrix}, \tag{3}$$

where ρ_0 is the condensate density and $\delta\rho(\mathbf{r},t)$, $\delta\theta(\mathbf{r},t)$, $\delta\phi(\mathbf{r},t)$, and $\delta\xi(\mathbf{r},t)$ are space-time dependent fluctuations.

We substitute Eq. (3) into (2) and then expand the resulting expression up to linear terms in the fluctuations, which gives

$$\partial_t\begin{bmatrix}\delta\rho(\mathbf{r},t)\\ \delta\theta(\mathbf{r},t)\\ \delta\phi(\mathbf{r},t)\\ \delta\xi(\mathbf{r},t)\end{bmatrix} = \begin{bmatrix}0 & -2\rho_0\nabla^2 & 0 & -2\lambda\rho_0\partial_y\\ -(-\nabla^2+m_v)/(2\rho_0) & 0 & 2\lambda\partial_y & 0\\ 0 & 2\lambda\partial_y & 4\lambda\partial_x & (-\nabla^2+4\lambda^2)/2\\ -2\lambda\partial_y/\rho_0 & 0 & -(-2\nabla^2+8\lambda^2) & 4\lambda\partial_x\end{bmatrix}\begin{bmatrix}\delta\rho(\mathbf{r},t)\\ \delta\theta(\mathbf{r},t)\\ \delta\phi(\mathbf{r},t)\\ \delta\xi(\mathbf{r},t)\end{bmatrix} - g_i\delta(\mathbf{r}-\mathbf{v}t)\begin{bmatrix}0\\1\\0\\0\end{bmatrix}. \tag{4}$$

Here m_v is the mass for $\delta\rho$ fluctuations, which equals $2g\rho_0$ in the classical limit [50]. The last term on the right-hand side of Eq. (4) shows that the impurity potential directly affects the global phase fluctuations $\delta\theta(\mathbf{r},t)$. When $g_{i\uparrow} \neq g_{i\downarrow}$, the impurity will also directly affect $\delta\xi(\mathbf{r},t)$, which are fluctuations of the relative phase between the two components of the bosons. It is not considered in this paper.

The drag force experienced by the impurity is [52]

$$\begin{aligned}\mathbf{F}(t) &= -\int |\Psi(\mathbf{r},t)|^2\nabla[g_i\delta(\mathbf{r}-\mathbf{v}t)]\,d^2\mathbf{r}\\ &= g_i[\nabla|\Psi(\mathbf{r},t)|^2]|_{\mathbf{r}=\mathbf{v}t}\\ &= g_i\int i\mathbf{k}\delta\rho(\mathbf{k},t)e^{i\mathbf{k}\cdot\mathbf{v}t}d^2\mathbf{k},\end{aligned} \tag{5}$$

where $\mathbf{k}$ is the kinetic momentum of a fluctuation over the condensate. The second line in Eq. (5) shows that the drag force is a measure of the density gradient around the impurity.

Let us now calculate $\delta\rho(\mathbf{k},t)$ from the linearized GP equation (4). We first perform a Fourier transformation to change the equation into momentum space. The evolutions of fluctuations with different momenta are decoupled in the linear GP equation. For a specified momentum $\mathbf{k}$, there is

$$\frac{\partial \mathbf{X}(\mathbf{k},t)}{\partial t} = \mathbf{A}(\mathbf{k})\mathbf{X}(\mathbf{k},t) + \mathbf{B}(\mathbf{k},t). \tag{6}$$

Here $\mathbf{X}(\mathbf{k},t) \equiv [\delta\rho(\mathbf{k},t),\delta\theta(\mathbf{k},t),\delta\phi(\mathbf{k},t),\delta\xi(\mathbf{k},t)]^T$. $\mathbf{A}(\mathbf{k})$ is a 4×4 matrix transformed from the one in Eq. (4). $\mathbf{B}(\mathbf{k},t)$ is a four-component vector obtained from a Fourier transform of the last term in Eq. (4). The differential equation (6) can be exactly solved as

$$\mathbf{X}(\mathbf{k},t) = e^{(t-t_0)\mathbf{A}(\mathbf{k})}\mathbf{X}(\mathbf{k},t_0) + \int_{t_0}^{t} e^{(t-s)\mathbf{A}(\mathbf{k})}\mathbf{B}(\mathbf{k},s)ds. \tag{7}$$

The matrix exponential $e^{t\mathbf{A}}$ in Eq. (7) is derived following the method in Ref. [53]. Details are given in Appendix A.

The first term on the right-hand side of Eq. (7) represents the evolution of the quantum fluctuations without the influence of the impurity potential. It gives zero contributions to the drag force (5). The second term on the right-hand side of Eq. (7) represents the evolution of the fluctuations induced by the impurity potential. It is proportional to g_i. So the drag force (5) depends quadratically on g_i, which is the same as that without SOC [52]. Let $t_0 = -\infty$ in Eq. (7) so as to turn on the impurity potential adiabatically. In this way, the system will be in a steady state.

Substituting the obtained density fluctuations $\delta\rho(\mathbf{k},t)$ into the drag force (5), and using analytic continuation to treat the Landau causality [52,54], we finally have

$$\mathbf{F} = -4\pi\rho_0 g_i^2 \int d^2\mathbf{k}\mathbf{k} \left\{ \frac{-D + (\omega_{\mathbf{k}}^+\omega_{-\mathbf{k}}^+ + \omega_{\mathbf{k}}^+\omega_{-\mathbf{k}}^- - \omega_{-\mathbf{k}}^+\omega_{-\mathbf{k}}^-)k^2}{(\omega_{-\mathbf{k}}^+ + \omega_{\mathbf{k}}^-)(\omega_{\mathbf{k}}^+ - \omega_{\mathbf{k}}^-)(\omega_{\mathbf{k}}^- + \omega_{-\mathbf{k}}^-)} \delta(\omega_{\mathbf{k}}^- - \mathbf{k}\cdot\mathbf{v}) \right.$$
$$\left. + \frac{D - (\omega_{-\mathbf{k}}^+\omega_{\mathbf{k}}^- + \omega_{\mathbf{k}}^-\omega_{-\mathbf{k}}^- - \omega_{-\mathbf{k}}^+\omega_{-\mathbf{k}}^-)k^2}{(\omega_{\mathbf{k}}^+ + \omega_{-\mathbf{k}}^+)(\omega_{\mathbf{k}}^+ + \omega_{-\mathbf{k}}^-)(\omega_{\mathbf{k}}^+ - \omega_{\mathbf{k}}^-)} \delta(\omega_{\mathbf{k}}^+ - \mathbf{k}\cdot\mathbf{v}) \right\}, \tag{8}$$

where $D = k^6 + 16\lambda^4 k_y^2 + 12\lambda^2 k^2 k_y^2 + m_v k^4$ and $\omega_{\mathbf{k}}^+$ and $\omega_{\mathbf{k}}^-$ are eigenenergies of excitations with momentum $\mathbf{k}$ in the upper and lower bands, respectively [50]. For momenta $\mathbf{k}$ satisfying $\omega_{\mathbf{k}}^+ = \omega_{\mathbf{k}}^-$, the coefficients before the two δ functions in Eq. (8) are exactly zero, and there are no contributions to the drag force from excitations with these momenta. So we can neglect the poles in Eq. (8).

The obtained $\delta\rho(\mathbf{k},t)$ has a factor $e^{-i\mathbf{k}\cdot\mathbf{v}t}$, which cancels the term $e^{i\mathbf{k}\cdot\mathbf{v}t}$ in Eq. (5). So the drag force (8) is time independent. It is consistent with the situation that the system is in a steady state. In addition, after a Fourier transformation, we find the density fluctuations created by the motion of the impurity have the form $\delta\rho(\mathbf{r}-\mathbf{v}t)$ in real space. In Ref. [52], this form of the density fluctuations is taken as an assumption in the calculations of the drag force in the case without SOC.

Using the method above, we can also obtain the drag force for the case without SOC as $\mathbf{F} = -2\pi\rho_0 g_i^2 \int d^2\mathbf{k}\mathbf{k}\frac{k^2}{\omega_{\mathbf{k}}}\delta(\omega_{\mathbf{k}} - \mathbf{k}\cdot\mathbf{v})$. It is the same as that in Ref. [52].

From the two δ functions in Eq. (8), we find that the excitations with momenta

$$\omega_{\mathbf{k}}^+ - \mathbf{k}\cdot\mathbf{v} = 0, \quad \text{or} \quad \omega_{\mathbf{k}}^- - \mathbf{k}\cdot\mathbf{v} = 0 \tag{9}$$

contribute to the drag force. The δ functions result from causality. The Landau criterion for a Galilean-invariant superfluid has two forms: When the impurity is moving and the superfluid is at rest, it is $\omega_{\mathbf{k}} - \mathbf{k}\cdot\mathbf{v} = 0$, whereas when the impurity is at rest and the superfluid is moving, it is $\omega_{\mathbf{k}} + \mathbf{k}\cdot\mathbf{v} = 0$ [29,55]. Our results (9) are the same as for the first form. In systems with inversion symmetry, there is $\omega_{\mathbf{k}} = \omega_{-\mathbf{k}}$. Then the two forms of the Landau criterion are the same. In a spin-orbit-coupled plane-wave BEC, the inversion symmetry is broken. It is interesting to ask whether the Landau criterion with $\omega_{\mathbf{k}} + \mathbf{k}\cdot\mathbf{v} = 0$ still applies when the superfluid moves past a resting impurity. This will be left to future considerations.

Let us now solve Eq. (9) to obtain the momenta of excitations induced by the motion of the impurity. The dispersions of excitations $\omega_{\mathbf{k}}$ satisfy [35,50]

$$\omega_{\mathbf{k}}^4 + b\omega_{\mathbf{k}}^3 + c\omega_{\mathbf{k}}^2 + d\omega_{\mathbf{k}} + e = 0, \tag{10}$$

where the coefficients are $b = 8\lambda k_x$, $c = -[16\lambda^4 + 8\lambda^2 k^2 - 16\lambda^2 k_x^2 + 8\lambda^2 k_y^2 + 2k^4 + m_v k^2]$, $d = -8\lambda k_x[4\lambda^2 k_y^2 + (k^2 + m_v)k^2]$, and $e = (k^4 - 4\lambda^2 k_x^2)^2 + m_v[k_x^2(k^2 - 4\lambda^2)^2 + k^2 k_y^2(k^2 + 4\lambda^2)]$. From Eqs. (9) and (10), we deduce that the desired momenta obey a necessary condition,

$$(\mathbf{k}\cdot\mathbf{v})^4 + b(\mathbf{k}\cdot\mathbf{v})^3 + c(\mathbf{k}\cdot\mathbf{v})^2 + d\mathbf{k}\cdot\mathbf{v} + e = 0. \tag{11}$$

In polar coordinates, we set the principal direction of the plane-wave condensate as $\theta = 0$ and denote the direction of the motion of the impurity as $\theta = \theta_0$. That is, $(k_x,k_y) = k(\cos\theta, \sin\theta)$ and $(v_x,v_y) = v(\cos\theta_0, \sin\theta_0)$. Equation (11) then becomes

$$k^6 + s_4 k^4 + s_2 k^2 + s_0 = 0, \tag{12}$$

where

$$\begin{aligned} s_4 &= -2[2\lambda\cos\theta + v\cos(\theta-\theta_0)]^2 + m_v, \\ s_2 &= [2\lambda\cos\theta + v\cos(\theta-\theta_0)]^4 \\ &\quad - 16\lambda^2 v\cos(\theta-\theta_0)[2\lambda\cos\theta + v\cos(\theta-\theta_0)] \\ &\quad + m_v\{-2[2\lambda\cos\theta + v\cos(\theta-\theta_0)] \\ &\quad \times [6\lambda\cos\theta + v\cos(\theta-\theta_0)] + 4\lambda^2\}, \\ s_0 &= -16\lambda^4 v^2\cos^2(\theta-\theta_0) + 16 m_v\lambda^4\cos^2\theta. \end{aligned} \tag{13}$$

Equation (12) is a cubic equation for k^2 when v, θ, and θ_0 are specified. So it can be solved analytically. Our methods to solve Eq. (9) are outlined as follows: We first solve the momenta from Eq. (12) with the constraints that $k > 0$ and $\mathbf{k}\cdot\mathbf{v} \geqslant 0$; whether the obtained momenta belong to the upper or lower band are determined by checking with Eq. (9). A short proof on the validity of the methods is given in Appendix B.

In polar coordinates, the integration $\int d^2\mathbf{k}$ in Eq. (8) is changed into $\int d\theta \int dk k$. The two δ functions in Eq. (8) are removed analytically by first employing the formula [56]

$$\delta(f(k)) = \sum_i \frac{1}{|f'(k)|_{k=k_i}}\delta(k-k_i) \tag{14}$$

and then doing an integration over k. The denominators in Eq. (14) are calculated using

$$\frac{\partial\omega_{\mathbf{k}}^{\pm}}{\partial k} = -\frac{\frac{\partial b}{\partial k}(\omega_{\mathbf{k}}^{\pm})^3 + \frac{\partial c}{\partial k}(\omega_{\mathbf{k}}^{\pm})^2 + \frac{\partial d}{\partial k}\omega_{\mathbf{k}}^{\pm} + \frac{\partial e}{\partial k}}{4(\omega_{\mathbf{k}}^{\pm})^3 + 3b(\omega_{\mathbf{k}}^{\pm})^2 + 2c\omega_{\mathbf{k}}^{\pm} + d}. \tag{15}$$

This equation is obtained by differentiating Eq. (10) with respect to $\mathbf{k}$. Since Eq. (10) is satisfied for any momentum $\mathbf{k}$, the differentiation of its left-hand side gives zero. This immediately leads to Eq. (15).

III. DRAG FORCE AND SUPERFLUID CRITICAL VELOCITY

In this section, we present the drag force $\mathbf{F}$ experienced by the moving impurity in the spin-orbit-coupled BEC. The superfluid critical velocity v_c is then derived.

In Fig. 2, we present the drag forces as a function of v/λ for some typical values of θ_0. We use F_L and F_T to denote the longitudinal and transverse components of the drag force, respectively. The result is

$$\begin{aligned} F_L &\equiv F_x\cos\theta_0 + F_y\sin\theta_0, \\ F_T &\equiv -F_x\sin\theta_0 + F_y\cos\theta_0. \end{aligned} \tag{16}$$

Since the boson system without the impurity is symmetric with respect to the k_x axis, we only need to consider the cases with $0 \leqslant \theta_0 \leqslant \pi$. We choose $\tilde{m}_v \equiv m_v/\lambda^2 = 1$ in Fig. 2. For different values of $\tilde{m}_v$, the behaviors of the drag forces are qualitatively the same, provided that the quantum fluctuations are weak.

In Table I, we have listed the characteristics of the v/λ dependence of the drag forces for different values of θ_0. The second row of the table states that the superfluid critical velocity v_c is nonzero only for $\theta_0 = \pi$, which has zero weight in the phase space of θ_0. The third row of the table says that there exists a nonzero transverse force for motion in directions $0 < \theta_0 < \pi$. The fourth row of the table states that the drag force is very tiny with a small v/λ for motion in directions $\pi/2 < \theta_0 < \pi$, while it is considerable in other directions. The fifth row shows that there is a jump in the drag force as v/λ varies for $0.27\pi \leqslant \theta_0 < \pi$. The lower bound $\theta_0 = 0.27\pi$ depends on the value of $\tilde{m}_v$, as shown in Fig. 3(a) for $10^{-2} \leqslant \tilde{m}_v \leqslant 10$, which is typical in ultracold atom experiments. The last row of the table states that, for $0 \leqslant \theta_0 < 0.65\pi$, there are nonanalytic peaks in the v/λ dependence of the drag forces. The upper bound $\theta_0 = 0.65\pi$ also depends on the value of $\tilde{m}_v$, as shown in Fig. 3(b).

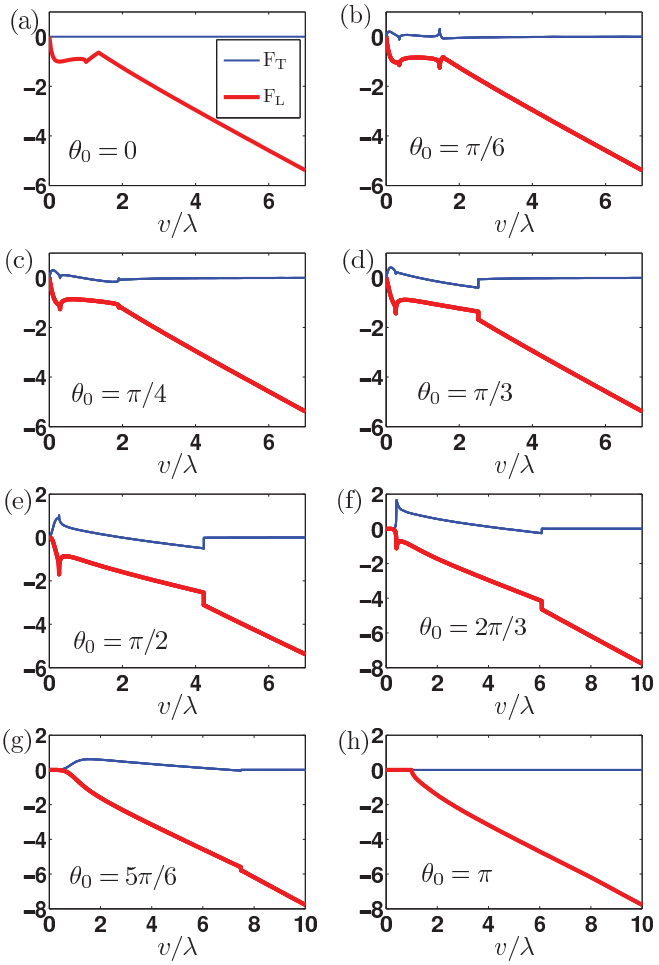

FIG. 2. (Color online) The v/λ dependence of the longitudinal (F_L) and transverse (F_T) drag forces experienced by the impurity. The drag forces are in the unit of $4\pi\rho_0 g_i^2\lambda$. We take $\equiv m_v/\lambda^2 = 1$ in our calculations. The characteristics of the drag force as θ_0 varies are summarized in Table I.

TABLE I. Classifications of the v/λ dependence of the drag force according to θ_0.

	θ_0		
v_c	$[0,\pi)$ $= 0$		$\{\pi\}$ > 0
Existence of a nonzero F_T	$\{0\}$ No	$(0,\pi)$ Yes	$\{\pi\}$ No
$\mathbf{F} \approx 0$ with a small v/λ	$[0,\pi/2]$ No	$(\pi/2,\pi)$ Yes	$\{\pi\}$ $F = 0$
Existence of a jump	$[0,0.27\pi)$[a] No	$[0.27\pi,\pi)$[a] Yes	$\{\pi\}$ No
Existence of peaks	$[0,0.65\pi]$[a] Yes		$(0.65\pi,\pi]$[a] No

[a]The values of the bounds 0.27π,0.65π depend on m_v/λ^2, as shown in Fig. 3. We take $m_v/\lambda^2 = 1$ in our calculations.

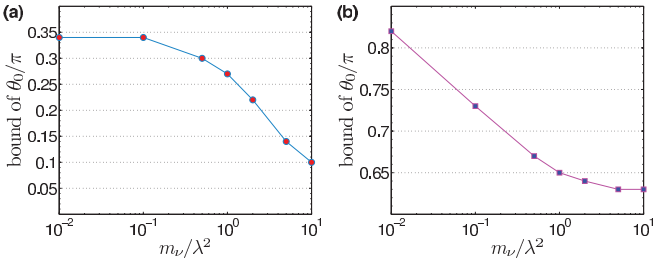

FIG. 3. (Color online) The m_v/λ^2 dependence of the bounds that appear in the last two rows of the Table I for (a) existence of a jump in the drag force and (b) existence of peaks in the drag force.

In addition to the results listed in Table I, we also have $F_T \simeq 0$ and $F_L \propto v/\lambda$ (in unit of $4\pi\rho_0 g_i^2\lambda$) with a large v/λ for any θ_0.

A. Superfluid critical velocity

As listed in the second row of Table I, the superfluid critical velocity v_c is nonzero only when the impurity moves in the direction $\theta_0 = \pi$. In the following we will prove this result analytically.

Since Eq. (12) is a cubic equation for k^2, it is easy to find that when the coefficient s_0 is negative, it has at least one positive root. It means that, when the value of v is specified, for any θ satisfies

$$s_0 = -16\lambda^4 v^2\cos^2(\theta-\theta_0) + 16 m_v\lambda^4\cos^2\theta < 0, \quad (17)$$

Equation (12) has solutions with a positive value. Equation (17), together with the constraint $\mathbf{k}\cdot\mathbf{v} \geqslant 0$, gives

$$\arctan\frac{\frac{\sqrt{m_v}}{v}-\cos\theta_0}{\sin\theta_0} < \theta < \pi - \arctan\frac{\frac{\sqrt{m_v}}{v}+\cos\theta_0}{\sin\theta_0}. \quad (18)$$

For convenience, in the above inequality, θ is defined in the region $[-\pi,\pi)$ when $0 < \theta_0 \leqslant \pi/2$, while it is defined in the region $[0,2\pi)$ when $\pi/2 < \theta_0 < \pi$. For any finite values of v and m_v, the inequality (18) covers a finite range of θ. This is because of the anisotropy of the Goldstone modes, which are softer than phonons with a linear dispersion. Since any excitation contributes a negative quantity to F_L, the total contributions from the excitations given by the inequality (18) are finite.

In addition to the Goldstone modes, there are always a collection of spin waves with momenta around $\mathbf{k} = (2\lambda,0)$ that are excited, when the impurity moves in directions $0 \leqslant \theta_0 \leqslant \pi/2$ with any finite v. This is because the spin waves go soft for momenta around $\mathbf{k} = (2\lambda,0)$.

Therefore, the superfluid critical velocity $v_c = 0$ for $0 \leqslant \theta_0 < \pi$. This is one of the main results in this work.

The appearance of both the anisotropic Goldstone modes with dispersions softer than phonons and the spin waves results from the spontaneous lifting of the infinite degeneracy of the ground states by quantum fluctuations, which is called the order-by-disorder mechanism [32,33].

B. Impurity valve

As listed in the fourth row of Table I, when v/λ is small, there is an enormous difference between the transports of the impurity starts from the two ends of the spin-orbit-coupled BEC: It experiences considerable drag force when it moves in the directions $0 < \theta_0 \leqslant \pi/2$, while in directions $\pi/2 < \theta_0 < \pi$ the drag force is tiny.

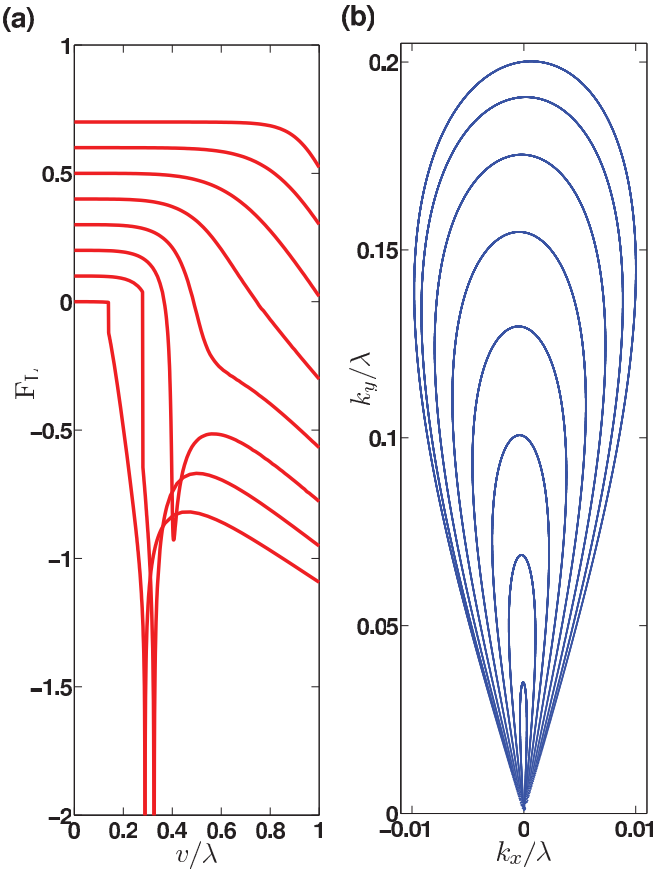

FIG. 4. (Color online) (a) F_L with a small v/λ for $\theta_0 = \pi/2 + j\pi/18$, $j = 1,2,\ldots,8$, from left to right. For clarity, the lines have been shifted upwards in steps as θ_0 increases. F_L are in the unit of $4\pi\rho_0 g_i^2\lambda$. F_L is tiny with a small v/λ. (b) The momenta of the excitations over the condensate due to the motion of the impurity for $v/\lambda = 0.1$ with θ_0 as in (a). The loops go large as θ_0 increases. The momenta of these Goldstone modes are quite small, which results in tiny drag forces.

The difference lies in the excitations of spin waves with a small v/λ only in the directions $0 < \theta_0 \leqslant \pi/2$, which give a large contribution to the drag force. Although Goldstone modes are excited by the impurity in both cases, their contributions to the drag force are tiny when the velocity of the impurity is small. This is illustrated in Fig. 4. In Fig. 4(a), we show the F_L with $0 < v/\lambda < 1$ for $\theta_0 = \pi/2 + j\pi/18, j = 1,2,\ldots,8$. The drag forces are quite small for all values of θ_0 with a small velocity, taking $v/\lambda = 0.1$ as an example. Figure 4(b) shows the momenta of excitations for all the θ_0 in Fig. 4(a) with $v/\lambda = 0.1$. Only Goldstone modes are excited, and their momenta are quite small. Furthermore, they compose a small phase space in momentum space. Simple calculations show that their contributions to the drag force are tiny.

These properties of the spin-orbit-coupled BEC imply the condensate can be employed as a potential impurity valve.

In applications, the principal direction of the condensate (or, equally, the momentum of condensate wave function) can be controlled by applying an infinitesimal magnetic field or a shift of the wavelength of the vector light coupled with the hyperfine states of ultracold atoms [26,57].

C. Transverse force

When the velocity of the impurity is not too large, generally the impurity experiences a finite transverse force, unless it moves along the symmetry axis of the condensate, as shown in Fig. 2. Moreover, the transverse force can reverse its direction when v/λ varies. When the velocity of the impurity is large enough, the transverse force becomes tiny for all θ_0. A sudden jump takes place in the transverse force when it becomes tiny for the motion of the impurity in directions $0.27\pi \leqslant \theta_0 < \pi$, while it evolves continuously for motion in directions $0 < \theta_0 < 0.27\pi$. We will focus on interpreting these properties in the following part of this subsection.

1. Transverse force with a small v/λ

For convenience, we write the drag force in Eq. (8) as $\mathbf{F} = \mathbf{F}^- + \mathbf{F}^+$, with

$$\begin{aligned} \mathbf{F}^- &\equiv -4\pi\rho_0 g_i^2 \int d^2\mathbf{k}\mathbf{k} f^-(\mathbf{k})\delta(\omega_{\mathbf{k}}^- - \mathbf{k}\cdot\mathbf{v}), \\ \mathbf{F}^+ &\equiv -4\pi\rho_0 g_i^2 \int d^2\mathbf{k}\mathbf{k} f^+(\mathbf{k})\delta(\omega_{\mathbf{k}}^+ - \mathbf{k}\cdot\mathbf{v}), \end{aligned} \tag{19}$$

where $f^{\pm}(\mathbf{k})$ denote corresponding factors before the δ functions.

The original Hamiltonian of the system (1) is symmetric with respect to the direction of $\mathbf{v}$. Naively, it implies zero F_T. However, the O(2) symmetry of the boson system in momentum space is broken by quantum fluctuations via selecting a single state from the macroscopic denegerate ground states when the Bose-Einstein condensation occurs. Only the symmetry with $k_y \leftrightarrow -k_y$ remains for the BEC system. This has the consequence that in Eq. (19) $\omega_{\mathbf{k}}^{\pm}$ are only symmetric under $k_y \leftrightarrow -k_y$, and $f^{\pm}(\mathbf{k})$ have only the inversion symmetry $\mathbf{k} \leftrightarrow -\mathbf{k}$, while $\mathbf{k}\cdot\mathbf{v}$ is symmetric with respect to the direction of $\mathbf{v}$. As a result, the expressions for $\mathbf{F}^{\pm}$ and also $\mathbf{F}$ are not symmetric with respect to the direction of $\mathbf{v}$. This can be seen more clearly for $\theta_0 = \pi/2$, in which the transverse force is along the symmetry axis of the condensate. In this case, there is

$$\begin{aligned} F_T = 4\pi\rho_0 g_i^2 \int_{-\infty}^{\infty} dk_x \int_0^{\infty} dk_y k_x [f^-(\mathbf{k})\delta(\omega_{\mathbf{k}}^- - k_y v) \\ + f^+(\mathbf{k})\delta(\omega_{\mathbf{k}}^+ - k_y v)]. \end{aligned} \tag{20}$$

Since $\omega_{\mathbf{k}}^{\pm}$ are not even functions of k_x [50], there is generally $F_T \neq 0$. In short, and merely from symmetry analysis, we find that the anisotropy of the BEC will generally lead to a nonzero transverse force.

In the following, we further take $\theta_0 = \pi/2$ as an example to investigate the properties of F_T and also the physical origins. In Fig. 5, we exhibit the momenta of the excited states for various values of v/λ.

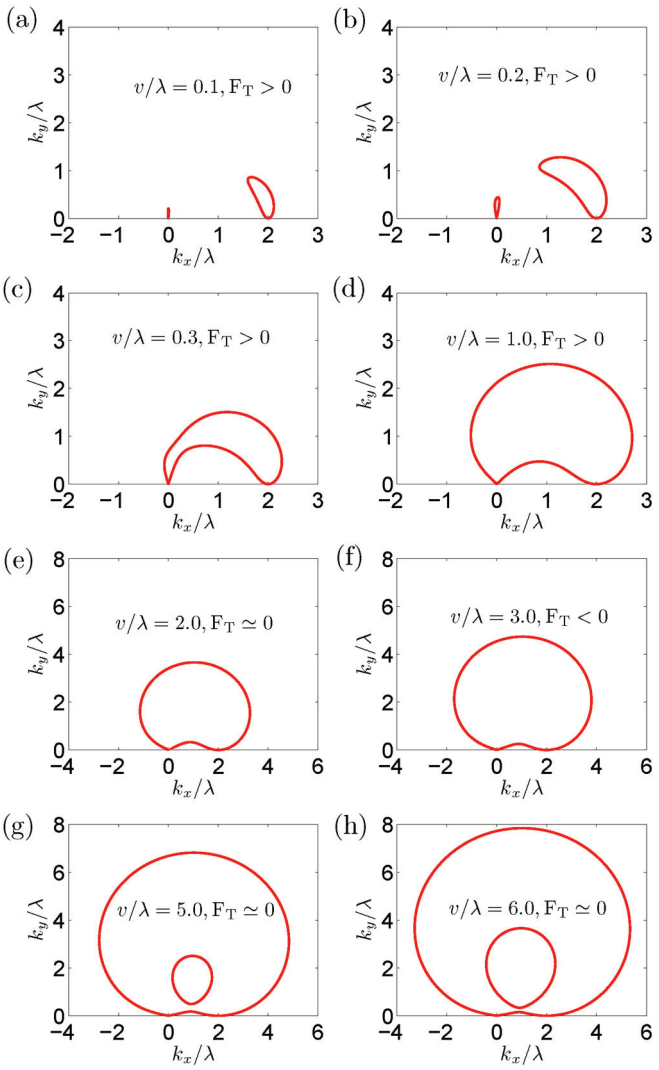

FIG. 5. (Color online) The momenta of excitations for $\theta_0 = \pi/2$ as v/λ increases. From (a) to (h), $v/\lambda = 0.1, 0.2, 0.3, 1.0, 2.0, 3.0, 5.0, 6.0$. In (a)–(c), the spin waves around $\mathbf{k} = (2\lambda, 0)$ dominate over the Goldstone modes around $\mathbf{k} = (0,0)$, and this leads to $F_T > 0$. From (d) to (f), the excitations with large momenta gradually dominate over the spin waves, and as a result, F_T changes continuously from positive to negative. In (g) and (h), the upper band (the smaller loops in the figures) also takes part, and the cancellation with the contributions from the lower band makes $F_T \simeq 0$.

With a small v/λ as in Figs. 5(a) and 5(b), the contour of the momenta is composed of two loops: One consists of Goldstone modes around the condensed momentum, and the other consists of spin waves around $\mathbf{k} = (2\lambda, 0)$. Only the states in the lower band are excited in Figs. 5(a) and 5(b). It is easy to see that the transverse force is mainly due to excitations of spin waves with a small v/λ, while the Goldstone modes give negligible contributions. First, in Eq. (20), $f^-(\mathbf{k}) \geqslant 0$ for any momentum $\mathbf{k}$, and for $\theta_0 = \pi/2$, the contribution to the transverse force by an excitation is proportional to k_x. k_x of the spin waves are around 2λ, which are large and always positive, whereas k_x of the Goldstone modes are quite small, and the contributions from the excitations with $k_x > 0$ and $k_x < 0$ will

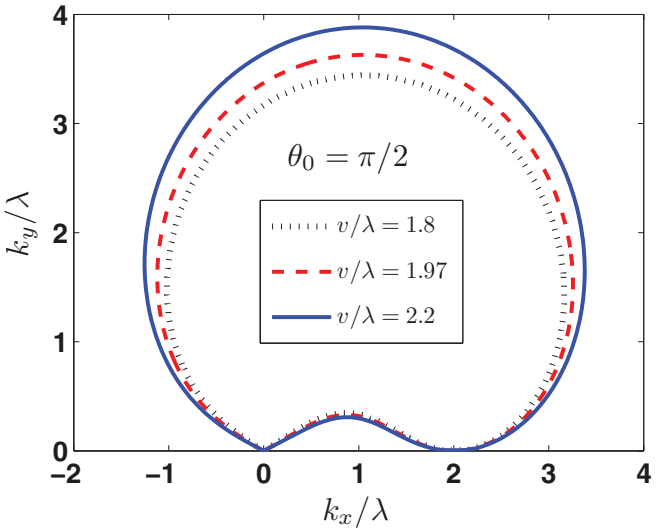

FIG. 6. (Color online) The momenta of excitations for $\theta_0 = \pi/2$ as v/λ increases, with the transverse force turning from positive to negative. There is the following: $F_T > 0$ for $v/\lambda = 1.8$; $F_T \simeq 0$ for $v/\lambda = 1.97$; $F_T < 0$ for $v/\lambda = 2.2$. The excitations with large momenta gradually dominate over the spin waves as v/λ increases.

further offset each other. Second, as shown clearly in Figs. 5(a) and 5(b), the phase space of the spin waves in momentum space is much larger than that of the Goldstone modes. From the above analysis, we conclude that with a small v/λ as in Figs. 5(a) and 5(b), the contributions to the drag force from the spin waves, which are positive, dominate over those from the Goldstone modes. As v/λ increases, the transverse force goes larger, since a larger number of spin waves are excited. This agrees with the result in Fig. 2(e).

When v/λ increases further, the two loops get larger, and then they merge into a single one, as shown in Fig. 5(c). The peak of F_T with $v/\lambda \simeq 0.27$ corresponds to the critical point when the two loops merge. The detailed analysis will be given in the Sec. III D.

After F_T goes over the peak point, it gradually decreases as v/λ increases. In the meantime, the loop gets larger. F_T decreases to approximately zero with v/λ about 2.0 (1.97 in precision) and then decreases continuously to negative. The contours in Figs. 5(d)–5(f) are similar in shape but differ in their sizes. In Fig. 6, we compare the contours of the momenta for $v/\lambda = 1.8, 1.97$, and 2.2. There is $F_T \simeq 0$ for $v/\lambda = 1.97$. There exist small differences among the parts with a small k_y in the three loops. The contributions of these parts to the transverse forces are almost the same. Spin waves dominate the part, so it provides a positive quantity to F_T. However, there are distinct differences among the parts with a large k_y in the three loops. The energies of the excitations in this part are large. The contributions to the transverse force from these states are given in Eq. (24) in the next subsection, which form a linear function of v/λ with a negative coefficient. So these states contribute a negative quantity to the transverse force, and this quantity decreases as v/λ goes from 1.8 to 2.0. Adding up the contributions from the two parts, we obtain that F_T is a decreasing function of v/λ within the range considered above, and it is possible that F_T will turn negative when v/λ is beyond some value (say $v/\lambda = 1.97$ for $\theta_0 = \pi/2$).

When v/λ increases further, as shown in Figs. 5(g) and 5(h), the upper band is also turned on, and F_T becomes tiny. It indicates that the two bands give opposite contributions to F_T. The physical origins of this result will be given in the remaining of this subsection.

2. *Drag force with a large v/λ*

With a large v/λ, there is $F_T \simeq 0$ and $F_L \propto v/\lambda$ (in unit of $4\pi\rho_0 g_i^2\lambda$), as shown in Fig. 2. To interpret this, we rewrite the drag force (8) as

$$\mathbf{F}(\lambda, m_v, \mathbf{v}) = v\tilde{\mathbf{F}}\left(\frac{\lambda}{v}, \frac{m_v}{v^2}, \frac{\mathbf{v}}{v}\right), \tag{21}$$

where $\tilde{\mathbf{F}}$ is the dimensionless form of $\mathbf{F}$ scaled by v. In the limit of large v/λ, there is $\lambda/v \simeq 0$, and $\tilde{\mathbf{F}}(\lambda/v, m_v/v, \mathbf{v}/v)$ has no manifest dependence on the SOC strength λ. Then the drag force $\mathbf{F} = v\tilde{\mathbf{F}}$ behaves like the one in the case without SOC, which has $F_T = 0$ and $F_L \propto v$ with a large v.

In the limit of large v/λ, $F_L^{\pm}$ and $F_T^{\pm}$ (in unit of $4\pi\rho_0 g_i^2\lambda$) are linear in v/λ for any θ_0. Two examples where $\theta_0 = \pi/2$ and $\pi/6$ are shown in Fig. 7. The two cases represent typical ones with and without a jump when the states in the upper band start to be excited, respectively. In Fig. 7, we find $F_L^{\pm} < 0$ and $F_T^{+} \simeq -F_T^{-} < 0$ with a large v/λ in both cases. These results turn out to be general for all $0 < \theta_0 < \pi$.

Let us now obtain the approximate behaviors of the drag force with a large v/λ by expanding it in powers of v/λ. The leading-order term is linear in v/λ. It is mainly contributed by states with large momenta, which are considered in the following calculations. The coefficient of the linear function will not be altered by neglecting the excitations with small momenta. The dispersions of excitations with large momenta are approximately $\omega_{\mathbf{k}}^{\pm} = (\sqrt{(k_x - \lambda)^2 + k_y^2} \pm \lambda)^2 + C^{\pm}(\mathbf{k})m_v + O(1/k)$, where $C^{\pm}(\mathbf{k})$ are anisotropic functions of $\mathbf{k}$ satisfying $0 \leqslant C^{\pm}(\mathbf{k}) \leqslant \frac{1}{2}$ and $C^{+}(\mathbf{k}) + C^{-}(\mathbf{k}) = \frac{1}{2}$ [58]. Substituting this into Eq. (8), we obtain the leading-order term of the drag force in powers of v/λ as

$$\mathbf{F} \simeq -4\pi\rho_0 g_i^2 \cdot \frac{1}{4}\int d^2\mathbf{k}\mathbf{k}\left[\left(1 - \frac{k_x}{k}\right)\delta(\omega_{\mathbf{k}}^{-} - \mathbf{k}\cdot\mathbf{v}) + \left(1 + \frac{k_x}{k}\right)\delta(\omega_{\mathbf{k}}^{+} - \mathbf{k}\cdot\mathbf{v})\right]. \tag{22}$$

The momenta that satisfy the δ functions $\delta(\omega_{\mathbf{k}}^{\pm} - \mathbf{k}\cdot\mathbf{v})$ are also solved in powers of v/λ. In polar coordinates, there is

$$k^{\pm} = \lambda\left[\cos(\theta - \theta_0)v/\lambda + 2(\cos\theta \mp 1) + O\left(\frac{1}{v/\lambda}\right)\right], \tag{23}$$

for a specified θ. Here, the possible values of θ are restricted by $k^{\pm} > 0$. After substituting this into Eq. (22) and performing the momentum integration, we finally obtain

$$F_L^{\pm} = -4\pi\rho_0 g_i^2\lambda\left\{\frac{1}{3}\left[\frac{3\pi}{8} \pm \cos\theta_0\right]v/\lambda + O((v/\lambda)^0)\right\},$$
$$F_T^{\pm} = \pm 4\pi\rho_0 g_i^2\lambda\left\{\frac{\sin\theta_0}{6}v/\lambda + O((v/\lambda)^0)\right\}. \tag{24}$$

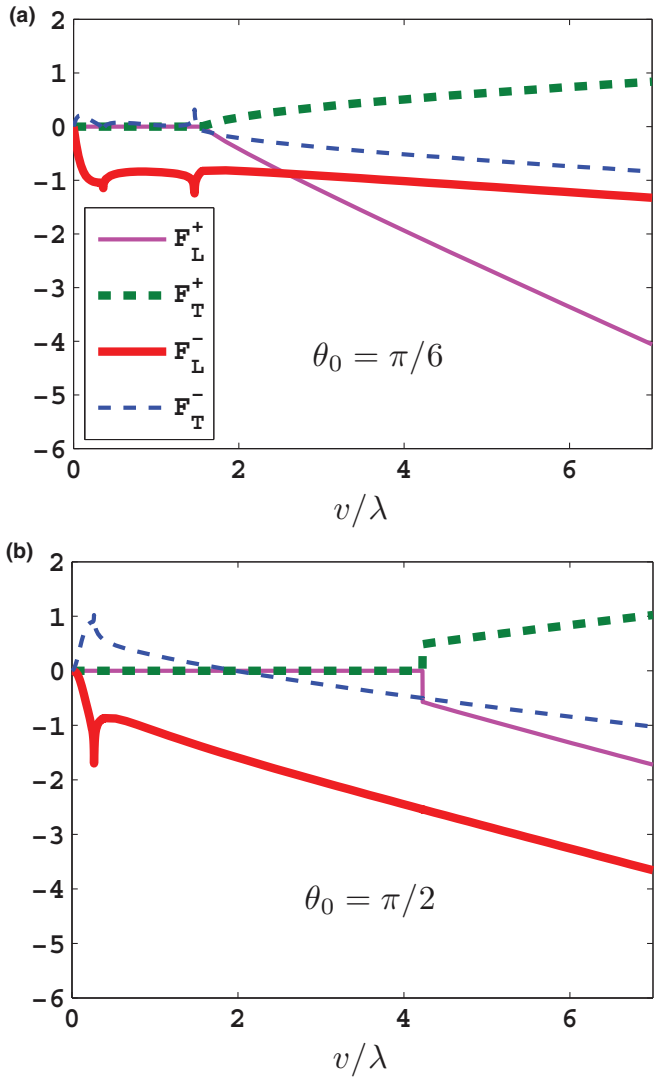

FIG. 7. (Color online) The drag forces (in unit of $4\pi\rho_0 g_i^2\lambda$) as a function of v/λ for (a) $\theta_0 = \pi/6$ and (b) $\theta_0 = \pi/2$. In (a) and (b), when v/λ is large, all of the lines are in linear of v/λ, and $F_T^+ \simeq -F_T^- > 0$. The jumps of F_L^+ and F_T^+ in (b) are due to turning on the excitations in the upper band, which give a finite contribution at the tangent point between the plane $\mathbf{k}\cdot\mathbf{v}$ and the band for $\omega_{\mathbf{k}}^+$. There is immediately $F_T = F_T^+ + F_T^- \simeq 0$. There are no jumps in (a) when the upper band starts to play a role, since the state at the touch point of the upper and lower bands are first excited, which gives a vanishing contribution.

The θ_0 dependence of the slopes of the linear functions in Eq. (24) are consistent with the ones in Fig. 7. The slopes for $F_L^{\pm}$ in Eq. (24) are negative for any θ_0. The sum of F_L^+ and F_L^- gives

$$F_L = -4\pi\rho_0 g_i^2\lambda\left\{\frac{\pi}{4}v/\lambda + O((v/\lambda)^0)\right\}. \tag{25}$$

The slope is θ_0 independent, which agrees with the results in Fig. 2. The terms $O((v/\lambda)^0)$ are approximately finite with a large v/λ, and they have an effect to shift the lines.

For any θ_0 in the region $0 < \theta_0 < \pi$, the slopes for F_T^+ and F_T^- in Eq. (24) are nonzero and opposite to each other. By adding F_T^+ and F_T^- together, we find the term of order $O((v/\lambda)^0)$ for F_T is exactly zero for any θ_0. The details are given in Appendix C. So there is

$$F_T = -4\pi\rho_0 g_i^2\lambda O\left(\frac{1}{v/\lambda}\right). \tag{26}$$

It is very small with a large v/λ, which is consistent with the results in Fig. 2.

To find out the physical origins for the behaviors of the transverse forces, we take $\theta_0 = \pi/2$ as an example. In this case, the slope of F_T^- in Eq. (24) is negative, which means that the total contributions of the excitations with large momenta to F_T^- are negative. It is consistent with the result in Fig. 5 that when v/λ becomes large, the value of the transverse force can be negative. In Eq. (22), only the terms $\pm\frac{k_x}{k}$ in the factors $1 \pm \frac{k_x}{k}$ give contributions to $F_T^{\pm}$ after performing the momentum integration. For $\theta_0 = \pi/2$, it means excitations with the same momentum, which is large, from the two bands give opposite contributions to the transverse force. It is explained as follows. First, in the free-boson system, the states in the upper and lower bands have opposite helicities [59], which are defined as the eigenvalues of the helicity operator $\hat{h} = \mathbf{k}\cdot\sigma/|\mathbf{k}|$. Second, in the interacting boson system, the excitations with large momenta behave like free bosons. Third, it is easy to find that exciting a single particle with definite helicity by a mobile impurity will induce a nonzero transverse force, the direction of which will be reversed if the sign of the helicity is changed. This helicity-dependent transverse force has also been detected in a recent experiment [60]. The physical origins given above for $\theta_0 = \pi/2$ are suitable for general cases.

3. *Jump in drag force as v/λ varies*

We find there is a finite jump in both F_L and F_T as v/λ varies for $0.27\pi \leqslant \theta_0 < \pi$, where the lower bound 0.27π depends on the value of m_v/λ^2 as shown in Fig. 3(a). The height of the hump evolves continuously to zero in other directions.

Let us now explain the appearance of the jump for $0.27\pi \leqslant \theta_0 < \pi$. In these cases when $v \geqslant v_{\rm th}$, where $v_{\rm th}$ denotes a θ_0-dependent threshold velocity, the states in the upper band begin to be excited by the impurity. When $v = v_{\rm th}$, only one state in the upper band is excited, the momentum of which is denoted as $\mathbf{k}_{\rm th} = k_{\rm th}(\cos\theta_{\rm th}, \sin\theta_{\rm th})$. It satisfies

$$\begin{aligned}\left.\frac{\partial\omega_{\mathbf{k}}^+}{\partial k}\right|_{k=k_{\rm th}} - v_{\rm th}\cos(\theta_{\rm th}-\theta_0) = 0,\\ \left.\frac{\partial\omega_{\mathbf{k}}^+}{\partial\theta}\right|_{\theta=\theta_{\rm th}} + k_{\rm th}v_{\rm th}\sin(\theta_{\rm th}-\theta_0) = 0.\end{aligned} \tag{27}$$

Its contribution to the drag force is

$$\begin{aligned}\mathbf{F}_{\rm th}^+ &= -4\pi\rho_0 g_i^2\int d^2\mathbf{k}\mathbf{k}f^+(\mathbf{k})\delta(\omega_{\mathbf{k}}^+ - \mathbf{k}\cdot\mathbf{v}_{\rm th})\\ &= -4\pi\rho_0 g_i^2\int d^2\mathbf{k}\mathbf{k}f^+(\mathbf{k})C\delta(k-k_{\rm th})\delta(\theta-\theta_{\rm th}),\end{aligned} \tag{28}$$

where C is a finite number proportional to the inverse of the curvature of function $\omega_{\mathbf{k}}^+ - \mathbf{k}\cdot\mathbf{v}_{\rm th}$ in momentum space. Since $\mathbf{k}_{\rm th}f^+(\mathbf{k}_{\rm th})$ in Eq. (28) is generally nonzero, $\mathbf{F}_{\rm th}^+$ gives a finite contribution to the drag force. It results in the jump in the drag force. Further, it is easy to prove that there is $\theta_{\rm th} \neq \theta_0$,

which means the induced drag force has a nonzero transverse component, see Fig. 7(b) for $\theta_0 = \pi/2$ as an example.

For the motion in direction $\theta_0 = \pi$, there exists a momentum that satisfies Eq. (27). However, it gives $f^+(\mathbf{k}_{\rm th}) = 0$, so the integration in Eq. (28) vanishes, which means that there is no jump in this case.

For motion in the directions $0 \leqslant \theta_0 < 0.27\pi$, when the velocity of the impurity increases, the state where the upper and lower bands touch is excited first, the momentum of which makes $f^+(\mathbf{k}) = 0$. As a result, no jump exists in these cases. See $\theta_0 = \pi/6$ in Fig. 7(a) as an example.

D. Peaks in drag force as a function of v/λ

We find for $0 \leqslant \theta_0 \leqslant 0.65\pi$ that there exist nonanalytic peaks in v/λ dependence of the drag forces. Here the upper bound 0.65π depends on the value of m_v/λ^2, as shown in Fig. 3(b). The nonanalytic behavior is because when v/λ varies, there exist topological changes in the contours for the momenta of the excited states in momentum space. The peak corresponds to the critical point when the number of the loops changes. See $\theta_0 = 5\pi/8$ in Figs. 8(a) and 8(c) as an example. Since the drag force is proportional to the gradient of the density of states in real space [see the second line in Eq. (5)], the peak structure means the density of states is a nonanalytic function of v/λ.

For $0.65 < \theta_0 \leqslant \pi$, no such topological change occurs as v/λ varies, and only analytic humps exist in v/λ dependence of the drag forces. See $\theta_0 = 5\pi/8$ in Figs. 8(b) and 8(d) as an example.

IV. CONCLUSIONS

In conclusion, we study a pointlike impurity moves with a constant velocity in a two-dimensional spin-orbit-coupled plane-wave Bose-Einstein condensate. We have calculated the drag force exerted on the impurity by the condensate and also the superfluid critical velocity based on a time-dependent Gross-Pitaevskii equation. We have proved rigorously that the superfluid critical velocity is zero for the motion of the impurity in all directions but one. This is because of the excitation of anisotropic Goldstone modes by the impurity. We find that there exists an enormous difference in the magnitude of the drag force for the impurity to be scattered into the plane-wave condensate from two opposite ends. The difference comes from the fact that there are spin-wave excitations in one case while there are no excitations of this type in the other case. We also find that for a mobile impurity with a velocity not large, it will experience a transverse force when it moves in all directions except two special ones. The transverse force is due to the anisotropy of the Bose-Einstein condensate. Both the spin waves and the helical high-energy states play crucial roles in inducing this force. When the impurity moves fast, states with large momenta in both the upper and lower bands are excited, which have opposite helicity. Their contributions to the transverse force cancel each other and result in a tiny value.

Experimentally, our results can be verified by scattering a heavy neutral molecule into the BEC cloud and detecting its track and velocity. The longitudinal drag force will slow down the motion of the impurity. The transverse force makes the track of impurity curve, and the sign of the force reflects the direction of the curvature. We assume the spin-orbit-coupled ^{87}Rb Bose-Einstein condensate is confined in a harmonic trap with oscillator frequencies $(f_x, f_y, f_z) = (50\ \text{Hz}, 50\ \text{Hz}, 1000\ \text{Hz})$. The size of the condensate in plane is about 4 μm. The density of the condensate is modulated to $2.4 \times 10^{10}\ \text{cm}^{-2}$, which corresponds to $m_v/\lambda^2 \simeq 1$. We consider a molecule with a mass about 10 times that for a ^{87}Rb atom, and the s-wave scattering length between the molecule and a ^{87}Rb atom about the same as that between two ^{87}Rb atoms. When it is scattered into the condensate in the direction $\theta_0 = \pi/2$ with velocity $v = 1\text{mm/s}$, which gives $v/\lambda = 0.5$, then, according to our calculations, the transverse deflection is about 40 nm. To have a delay time up to 10% of that needed for an impurity to pass through the condensate without friction, the density of bosons should be at least $2.4 \times 10^{11}\ \text{cm}^{-2}$.

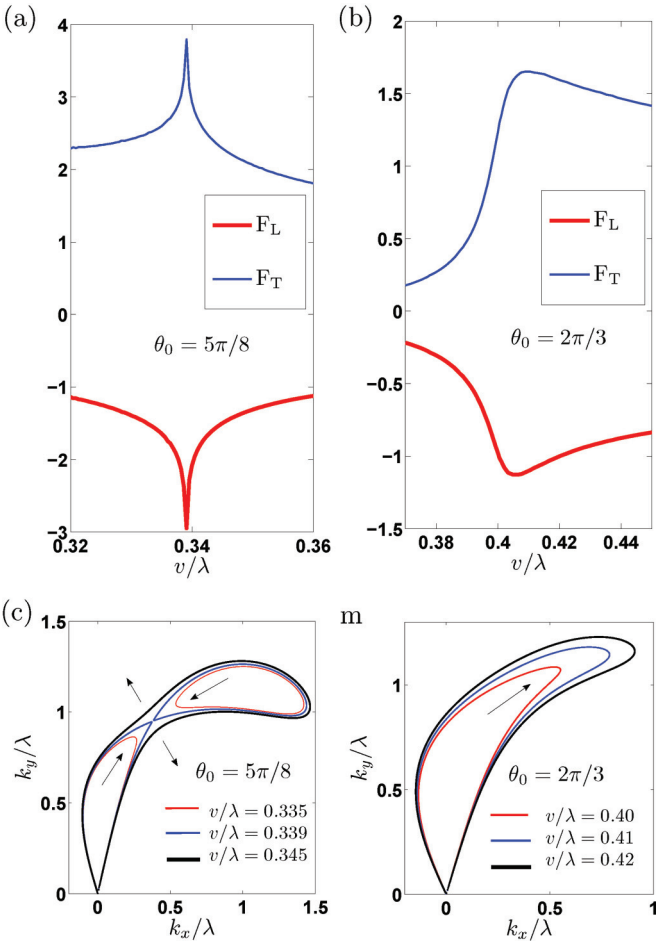

FIG. 8. (Color online) (a) Nonanalytic peaks and (b) analytic humps in drag forces as a function of v/λ. (c) The contour of momenta of excitations changes topologically from two loops to one loop when v/λ varies across the peak in (a). The peak corresponds to the critical point when two loops merge into a single one. The arrows indicate the evolution direction of the contour as v/λ increases. (d) The contour of the momenta of excitations evolves without a topological change when v/λ varies across the local minimum of the hump in (b).

ACKNOWLEDGMENTS

This work was supported by the National Key Basic Research Special Foundation of China (NKBRSFC) under Grants No. 2011CB921502 and No. 2012CB821305; the National Natural Science Foundation of China (NSFC) under Grants No. 61227902, No. 61378017, No. 11174020, and No. 11075176; the Beijing Natural Science Foundation (BNSF) under Grants No. 2102014 and No. 1112007; the Starting up Foundation for Youth Teachers of Beijing Technology and Business University under Grants No. QNJJ20123-19 and No. QNJJ2012-33; and the Project Sponsored by the Scientific Research Foundation for the Returned Overseas Chinese Scholars, State Education Ministry, Funding for Training Talents in Beijing City with Projects No. 2011D005003000012 and No. PXM2013-014213-000013; and the Importation and Development of High-Caliber Talents Project of Beijing Municipal Institutions No. CIT&TCD201404030.

APPENDIX A: MATRIX EXPONENTIAL $e^{t\mathbf{A}}$

In this appendix, we give the details of the calculations of the matrix exponential $e^{t\mathbf{A}}$ in Eq. (7).

The four eigenvalues of the matrix $\mathbf{A}$ in Eq. (6) are $\lambda_j = -i\omega_{\mathbf{k}}^{(j)}, j = 1,2,3,4$, where $\omega_{\mathbf{k}}^{(j)}$ are four roots of Eq. (10), $-\omega_{-\mathbf{k}}^{-}$, $-\omega_{-\mathbf{k}}^{+}$, $\omega_{\mathbf{k}}^{+}$, and $\omega_{\mathbf{k}}^{-}$. Following the method in Ref. [53], the exponential of matrix $\mathbf{A}$ is

$$e^{t\mathbf{A}} = \varphi_1(t)\mathbf{I} + \varphi_2(t)\mathbf{A} + \varphi_2(t)\mathbf{A}^2 + \varphi_3(t)\mathbf{A}^3. \tag{A1}$$

Here

$$\begin{aligned}&[\varphi_1(t)\varphi_2(t)\ \varphi_3(t)\ \varphi_4(t)]\\ &\quad= [y_1(t)\ y_2(t)\ y_3(t)\ y_4(t)]\mathbf{W}[y;0]^{-1},\end{aligned} \tag{A2}$$

and $y_j(t) = e^{\lambda_j t}, j = 1,2,3,4$. $\mathbf{I}$ is the 4×4 unit matrix. $\mathbf{W}[y;t]$ is the Wronski matrix,

$$\mathbf{W}[y;t] = \begin{bmatrix} y_1(t) & y_2(t) & y_3(t) & y_4(t) \\ y_1'(t) & y_2'(t) & y_3'(t) & y_4'(t) \\ y_1''(t) & y_2''(t) & y_3''(t) & y_4''(t) \\ y_1'''(t) & y_2'''(t) & y_3'''(t) & y_4'''(t) \end{bmatrix}. \tag{A3}$$

From Eqs. (A1)–(A3), the drag force is

$$\begin{aligned}\mathbf{F}(t) &= g_i \int i\mathbf{k} d^2\mathbf{k}\delta\rho(\mathbf{k},t)e^{i\mathbf{k}\cdot\mathbf{v}t}\\ &= -4\pi\rho_0 g_i^2 \int d^2\mathbf{k} i\mathbf{k}\int_0^\infty ds[e^{s\mathrm{A}}]_{12}e^{i\mathbf{k}\cdot\mathbf{v}s},\end{aligned} \tag{A4}$$

where

$$\begin{aligned}[e^{t\mathbf{A}}]_{1,2} = \sum_{j=1}^{4} y_j(t)\{&\mathbf{A}_{1,2}[\mathbf{W}[y;0]^{-1}]_{j,2}\\ &+[\mathbf{A}^2]_{1,2}[\mathbf{W}[y;0]^{-1}]_{j,3}\\ &+[\mathbf{A}^3]_{1,2}[\mathbf{W}[y;0]^{-1}]_{j,4}\}.\end{aligned} \tag{A5}$$

This gives the result in Eq. (8).

APPENDIX B: METHOD TO SOLVE THE MOMENTA OF EXCITATIONS

In this appendix, we will give a short proof on the validity of the method to solve Eq. (9) in Sec. II B.

First, for a specified momentum $\mathbf{k}$, Eq. (10) gives four roots, $\omega_{\mathbf{k}}^{\pm}$, $-\omega_{-\mathbf{k}}^{\pm}$. The detailed expressions are given in Ref. [50]. Second, we obtain the momentum $\mathbf{k}$ of an excitation induced by the moving impurity by solving Eq. (11) under the constraint that $k > 0$. Then we substitute this momentum into the four expressions of $\omega_{\mathbf{k}}^{\pm}$, $-\omega_{-\mathbf{k}}^{\pm}$. The results are represented as $\omega_{\mathbf{k}}^{(i)}, (i = 1,2,3,4)$. Finally, we substitute $\omega_{\mathbf{k}}^{(i)}, (i = 1,2,3,4)$ into Eq. (10) and subtract Eq. (11). The results are

$$\begin{aligned}&\left(\omega_{\mathbf{k}}^{(i)} - \mathbf{k}\cdot\mathbf{v}\right)\left\{\left(\omega_{\mathbf{k}}^{(i)} + \mathbf{k}\cdot\mathbf{v}\right)\left[\left(\omega_{\mathbf{k}}^{(i)}\right)^2 + \left(\mathbf{k}\cdot\mathbf{v}\right)^2\right]\right.\\ &\quad + b\left[\left(\omega_{\mathbf{k}}^{(i)}\right)^2 + \omega_{\mathbf{k}}^{(i)}(\mathbf{k}\cdot\mathbf{v}) + (\mathbf{k}\cdot\mathbf{v})^2\right]\\ &\quad \left.+ c\left(\omega_{\mathbf{k}}^{(i)} + \mathbf{k}\cdot\mathbf{v}\right) + d\right\} = 0, \quad (i = 1,2,3,4).\end{aligned} \tag{B1}$$

Since $\omega_{\mathbf{k}}^{(i)}, (i = 1,2,3,4)$ all differ from each other, for a specified $\mathbf{k}$ there exists only one $\omega_{\mathbf{k}}^{(i)}$ that makes $\omega_{\mathbf{k}}^{(i)} - \mathbf{k}\cdot\mathbf{v} = 0$. It equals $\omega_{\mathbf{k}}^{+}$ or $\omega_{\mathbf{k}}^{-}$, since there is $\mathbf{k}\cdot\mathbf{v} \geqslant 0$.

APPENDIX C: TRANSVERSE FORCE UP TO ORDER $O((v/\lambda)^0)$ AT LARGE v/λ

We give the details of calculating of transverse force $\mathrm{F_T}$ up to order $O((v/\lambda)^0)$ with a large v/λ as shown in Eq. (26).

From Eqs. (8) and (16), the transverse force is

$$\begin{aligned}F_T &= -F_x\sin\theta_0 + F_y\cos\theta_0\\ &= -4\pi\rho_0 g_i^2\int d\theta\sin(\theta-\theta_0)[k^- f^-(k^-,\theta)\\ &\quad + k^+ f^+(k^+,\theta)],\end{aligned} \tag{C1}$$

where $f^{\pm}(k^{\pm},\theta)$ are defined in Eq. (19) and $k^{\pm}$ are given by Eq. (23). By expanding $f^{\pm}(k^{\pm},\theta)$ in powers of $1/k^{\pm}$ at large $k^{\pm}$, we obtain

$$\begin{aligned}f^+(k^+,\theta) &= a_0^+ + a_1^+\frac{1}{k^+} + O\left[\frac{1}{(k^+)^2}\right],\\ f^-(k^-,\theta) &= a_0^- + a_1^-\frac{1}{k^-} + O\left[\frac{1}{(k^-)^2}\right],\end{aligned} \tag{C2}$$

where $a_0^{\pm}$ and $a_1^{\pm}$ are coefficients need to be calculated.

Using the expansion of dispersions at large momentum $\omega_{\mathbf{k}}^{\pm} = [\sqrt{(k_x-\lambda)^2+k_y^2} \pm \lambda]^2 + C^{\pm}(\mathbf{k})m_v + O(1/k)$, we obtain

$$\begin{aligned}f^+(k,\theta) &= \frac{A^+k^5 + B^+k^4 + O(k^3)}{C^+k^5 + D^+k^4 + O(k^3)},\\ f^-(k,\theta) &= \frac{A^-k^5 + B^-k^4 + O(k^3)}{C^-k^5 + D^-k^4 + O(k^3)},\end{aligned} \tag{C3}$$

where the coefficients are

$$\begin{aligned}A^{\pm} &= 4\lambda(1\pm\cos\theta),\\ C^{\pm} &= 16\lambda,\\ B^+ + B^- - \tfrac{1}{4}(D^+ + D^-) &= 16\lambda^2\cos\theta,\\ D^+ - D^- &= 64\lambda^2.\end{aligned} \tag{C4}$$

From Eqs. (C3) and (C4), we have

$$\begin{aligned} a_0^{\pm} &= \tfrac{1}{4}(1 \pm \cos\theta), \\ a_1^{+} + a_1^{-} &= 0. \end{aligned} \tag{C5}$$

By combining Eqs. (C1), (C2), and (C5), we find the term of order $O((v/\lambda)^0)$ in F_T is exactly zero for any θ_0. So the result can be written as

$$F_T = -4\pi\rho_0 g_i^2 \lambda O\left(\frac{1}{v/\lambda}\right). \tag{C6}$$

[1] I. Žutić, J. Fabian, and S. Das Sarma, Rev. Mod. Phys. **76**, 323 (2004).
[2] B. A. Bernevig and S.-C. Zhang, Phys. Rev. Lett. **96**, 106802 (2006).
[3] X.-L. Qi and S.-C. Zhang, Rev. Mod. Phys. **83**, 1057 (2011).
[4] M. Z. Hasan and C. L. Kane, Rev. Mod. Phys. **82**, 3045 (2010).
[5] A. M. Dudarev, R. B. Diener, I. Carusotto, and Q. Niu, Phys. Rev. Lett. **92**, 153005 (2004).
[6] J. Ruseckas, G. Juzeliūnas, P. Öhberg, and M. Fleischhauer, Phys. Rev. Lett. **95**, 010404 (2005).
[7] G. Juzeliūnas, J. Ruseckas, and J. Dalibard, Phys. Rev. A **81**, 053403 (2010).
[8] T. D. Stanescu, C. Zhang, and V. Galitski, Phys. Rev. Lett. **99**, 110403 (2007).
[9] Y. J. Lin, K. Jiménez-García, and I. B. Spielman, Nature (London) **471**, 83 (2011).
[10] J. Y. Zhang, S. C. Ji, Z. Chen, L. Zhang, Z. D. Du, B. Yan, G. S. Pan, B. Zhao, Y. J. Deng, H. Zhai, S. Chen, and J. W. Pan, Phys. Rev. Lett. **109**, 115301 (2012).
[11] P. Wang, Z. Q. Yu, Z. Fu, J. Miao, L. Huang, S. Chai, H. Zhai, and J. Zhang, Phys. Rev. Lett. **109**, 095301 (2012).
[12] L. W. Cheuk, A. T. Sommer, Z. Hadzibabic, T. Yefsah, W. S. Bakr, and M. W. Zwierlein, Phys. Rev. Lett. **109**, 095302 (2012).
[13] R. A. Williams, L. J. LeBlanc, K. Jiménez-García, M. C. Beeler, A. R. Perry, W. D. Phillips, and I. B. Spielman, Science **335**, 314 (2012).
[14] T. D. Stanescu, B. Anderson, and V. Galitski, Phys. Rev. A **78**, 023616 (2008).
[15] C. Wu and I. Mondragon-Shem, Chin. Phys. Lett. **28**, 097102 (2011).
[16] M. Merkl, A. Jacob, F. E. Zimmer, P. Öhberg, and L. Santos, Phys. Rev. Lett. **104**, 073603 (2010).
[17] S. Gopalakrishnan, A. Lamacraft, and P. M. Goldbart, Phys. Rev. A **84**, 061604(R) (2011).
[18] T. Ozawa and G. Baym, Phys. Rev. A **85**, 013612 (2012).
[19] C. Wang, C. Gao, C. M. Jian, and H. Zhai, Phys. Rev. Lett. **105**, 160403 (2010).
[20] T. Ozawa and G. Baym, Phys. Rev. A **84**, 043622 (2011).
[21] K. Zhou and Z. Zhang, Phys. Rev. Lett. **108**, 025301 (2012).
[22] C. M. Jian and H. Zhai, Phys. Rev. B **84**, 060508(R) (2011).
[23] L. Zhang, J. Y. Zhang, S. C. Ji, Z. D. Du, H. Zhai, Y. J. Deng, S. Chen, P. Zhang, and J. W. Pan, Phys. Rev. A **87**, 011601(R) (2013).
[24] X. Q. Xu and J. H. Han, Phys. Rev. Lett. **107**, 200401 (2011).
[25] X. F. Zhou, J. Zhou, and C. Wu, Phys. Rev. A **84**, 063624 (2011).
[26] J. Radić, T. A. Sedrakyan, I. B. Spielman, and V. Galitski, Phys. Rev. A **84**, 063604 (2011).
[27] Y. Deng, J. Cheng, H. Jing, C. P. Sun, and S. Yi, Phys. Rev. Lett. **108**, 125301 (2012).
[28] T. Graß, K. Saha, K. Sengupta, and M. Lewenstein, Phys. Rev. A **84**, 053632 (2011).
[29] E. M. Lifshitz and L. P. Pitaevskii, *Landau and Lifshitz Course of Theoretical Physics: Statistical Physics* (Butterworth-Heinemann, Oxford, 1980), Pt. 2.
[30] T. Ellis and P. V. E. McClintock, PhiL. Trans. R. Soc. A **315**, 259 (1985).
[31] C. Raman, M. Köhl, R. Onofrio, D. S. Durfee, C. E. Kuklewicz, Z. Hadzibabic, and W. Ketterle, Phys. Rev. Lett. **83**, 2502 (1999).
[32] J. Villain, R. Bidaux, J. P. Carton, and R. Conte, J. Phys. (France) **41**, 1263 (1980).
[33] R. Barnett, S. Powell, T. Graß, M. Lewenstein, and S. Das Sarma, Phys. Rev. A **85**, 023615 (2012).
[34] T. Ozawa and G. Baym, Phys. Rev. Lett. **109**, 025301 (2012).
[35] P. S. He, W. L. You, and W. M. Liu, Phys. Rev. A **87**, 063603 (2013).
[36] Q. Zhou and X. Cui, Phys. Rev. Lett. **110**, 140407 (2013).
[37] Y. Li, G. I. Martone, L. P. Pitaevskii, and S. Stringari, Phys. Rev. Lett. **110**, 235302 (2013).
[38] R. W. Ruhwandl and E. M. Terentjev, Phys. Rev. E **54**, 5204 (1996).
[39] H. Stark and D. Ventzki, Phys. Rev. E **64**, 031711 (2001).
[40] J. Loudet, P. Hanusse, and P. Poulin, Science **306**, 1525 (2004).
[41] T. Winiecki, J. F. McCann, and C. S. Adams, Phys. Rev. Lett. **82**, 5186 (1999).
[42] S. Sinha, R. Nath, and L. Santos, Phys. Rev. Lett. **107**, 270401 (2011).
[43] H. Hu, B. Ramachandhran, H. Pu, and X. J. Liu, Phys. Rev. Lett. **108**, 010402 (2012).
[44] B. Ramachandhran, B. Opanchuk, X. J. Liu, H. Pu, P. D. Drummond, and H. Hu, Phys. Rev. A **85**, 023606 (2012).
[45] T. Kawakami, T. Mizushima, M. Nitta, and K. Machida, Phys. Rev. Lett. **109**, 015301 (2012).
[46] S. W. Su, I. K. Liu, Y. C. Tsai, W. M. Liu, and S. C. Gou, Phys. Rev. A **86**, 023601 (2012).
[47] A. Aftalion and P. Mason, Phys. Rev. A **88**, 023610 (2013).
[48] A. Messiah, *Quantum Mechanics* (North-Holland, Amsterdam, 1961).
[49] Q. Zhu, C. Zhang, and B. Wu, Eur. Phys. Lett. **100**, 50003 (2012).
[50] P. S. He, R. Liao, and W. M. Liu, Phys. Rev. A **86**, 043632 (2012).
[51] W. Zheng and Z. Li, Phys. Rev. A **85**, 053607 (2012).
[52] G. E. Astrakharchik and L. P. Pitaevskii, Phys. Rev. A **70**, 013608 (2004).
[53] W. A. Harris, J. J. P. Fillmoe, and D. R. Smith, SIAM Rev. **43**, 694 (2001).

[54] Y. K. Lim and H. J. Lee, Open Plasma Phys. J. **5**, 36 (2012).
[55] M. Ueda, *Fundamentals and New Frontiers of Bose-Einstein Condensation* (World Scientific, Singapore, 2010).
[56] W. Appel, *Mathematics for Physics and Physicists* (Princeton University Press, Princeton, NJ, 2007).
[57] Y. J. Lin, R. L. Compton, K. Jimenez-Garcia, J. V. Porto, and I. B. Spielman, Nature **462**, 628 (2009).
[58] The explicit expressions of $C^{\pm}(\mathbf{k})$ are complicated and cannot yet be obtained by the authors. However, the relation $C^{+}(\mathbf{k}) + C^{-}(\mathbf{k}) = 1$ is proved as in Ref. [35], and it is suffices to use this relation alone to obtain the results in this work, especially the ones in Appendix C.
[59] H. Zhai, Int. J. Mod. Phys. B **26**, 1230001 (2012).
[60] H. Ikegami, Y. Tsutsumi, and K. Kono, Science **341**, 59 (2013).